

# Deconfining Phase Boundary of Rapidly Rotating Hot and Dense Matter and Analysis of Moment of Inertia

Yuki Fujimoto<sup>a</sup>, Kenji Fukushima<sup>a</sup>, Yoshimasa Hidaka<sup>b,c,d</sup>

<sup>a</sup>*Department of Physics, The University of Tokyo, 7-3-1 Hongo, Bunkyo-ku, Tokyo 113-0033, Japan*

<sup>b</sup>*Institute of Particle and Nuclear Studies, KEK, 1-1 Oho, Tsukuba, Ibaraki 305-0801 Japan*

<sup>c</sup>*Graduate University for Advanced Studies (Sokendai), Tsukuba 305-0801, Japan*

<sup>d</sup>*RIKEN iTHEMS, RIKEN, 2-1 Hirosawa, Wako, Saitama 351-0198, Japan*

---

## Abstract

We discuss the effect of rapid rotation on the phase diagram of hadronic matter. The energy dispersion relation is shifted by an effective chemical potential induced by rotation. This suggests that rotation should lower the critical temperature of chiral restoration, but it is still controversial how the deconfinement temperature should change as a function of angular velocity. We adopt the hadron resonance gas model as an approach free from fitting parameters. We identify the deconfinement from the thermodynamic behavior and find that rotation decreases the deconfinement temperature. We also discuss the spatial inhomogeneity of the pressure and give a semi-quantitative estimate of the moment of inertia.

*Keywords:* hadronic matter, quarks and gluons, phase transition, deconfinement, rotation

---

## 1. Introduction

Rotation effects are ubiquitous in various systems and have been one of the central topics in nuclear physics. A prominent example is the successful classification of nuclear spectra by the collective rotational modes. Some heavy nuclei spontaneously break rotational symmetry by deformation and rotate to restore the broken symmetry leading to the rotational band. A classic review is found in Ref. [1]; see also Ref. [2] for a modernized picture.

The present work addresses a nuclear system with more rapid rotation and higher temperature created in non-central relativistic heavy-ion collisions (see Refs. [3–5] for recent reviews). In the experiment a nonzero value of  $\Lambda$  and  $\bar{\Lambda}$  polarization has been confirmed and the observed polarization is translated to an angular velocity or vorticity  $\omega$  of created matter as large as  $\omega \simeq (9 \pm 1) \times 10^{21} \text{ s}^{-1}$  [6]. Some theoretical studies imply even higher values for vorticity [7–9]. Although expected  $\omega$  values are extraordinarily large, the corresponding energy scale is  $\omega \sim 6 \text{ MeV}$  in natural units. Still, in addition to the temperature  $T$ , the baryon chemical potential  $\mu$ , and the magnetic field  $B$ , the vorticity  $\omega$  plays a role as a relevant parameter to characterize the properties of hot and dense matter in heavy-ion collision phenomenology. Now, a lot of theoretical efforts are aimed to establish a full dynamical description of the polarization in terms of hydrodynamics or kinetic theory (see Refs. [4, 5] and references therein).

Apart from phenomenology, the rotation has been also interested from the wider point of view of quantum field theory or quantum chromodynamics (QCD). A well-known example is an anomalous transport phenomenon; namely, the chiral vortical effect [10–13]. Another interesting possibility is an exotic ground state such as the charged pion condensation emerging from a combination of rotation and magnetic field [14, 15]. Then, it is a natural anticipation that  $\omega$  should be a useful probe to investigate the QCD phase diagram. In theory  $\omega$  could be chosen to be comparable to a typical QCD scale, and it would be a quite inspiring question how the QCD phase diagram evolves with increasing  $\omega$ . In fact, the chiral phase transition has been already examined extensively in the literature [16–22]. It is a more or less accepted consensus that the rotation effect suppresses the chiral condensate just like the finite density effect, so that the chiral critical temperature drops with increasing  $\omega$ .

While most of the works have been concentrated on the chiral aspects, the deconfinement transition in QCD is recently being focused [23–25]. One of the latest lattice-QCD calculations, which builds upon the formulation in Ref. [26], claims that the deconfinement temperature,  $T_c$ , increases with growing  $\omega$  by measuring the Polyakov loop on the lattice in rotating frames [23]. A holographic QCD approach, by contrast, suggests the opposite behavior, i.e.,  $T_c$  decreases with growing  $\omega$  [24], which is in accordance with the behavior of the chiral critical temperature. There is also an alternative proposal of a mixed inhomogeneous phase supporting spatially separated confinement and deconfinement sectors [25].

---

*Email addresses:* fujimoto@nt.phys.s.u-tokyo.ac.jp

(Yuki Fujimoto), fuku@nt.phys.s.u-tokyo.ac.jp

(Kenji Fukushima), hidaka@post.kek.jp (Yoshimasa Hidaka)

In the present work we perform a simple yet robust analysis based on the hadron resonance gas (HRG) model to estimate thermodynamic quantities in a rotating frames. This model has no free parameter adjustable by hand and the input variables are all fixed by experimentally observed particle spectra. The virtue of the HRG model lies in its unambiguousness of the minimal model definition. The HRG model (or the thermal model fit) has manifested eminent successes in reproducing the particle abundances in heavy-ion collision experiments [27]. Furthermore, the HRG model has been found to be consistent with thermodynamic properties measured in lattice-QCD simulations up to  $\sim T_c$  or even for higher  $T$  once interactions are included [28, 29]. The ideal (i.e., non-interacting) HRG model prevails as long as we stay below  $T_c$ , but for  $T > T_c$  the thermodynamic quantities predicted from the ideal HRG model blow up. The breakdown of such a hadronic model based on the Hagedorn picture [30] should be identified as the deconfinement transition [31]. We will discuss this characterization later (see Ref. [32] for more details).

To this end we formulate how to calculate the pressure in the rotating frame. With global rotation the pressure is inhomogeneous to be balanced with the centrifugal force, from which we can infer the distribution of the angular momentum and also the moment of inertia of hot and dense matter. Our numerical results agree with empirical dependence on the radial distance from the rotation axis, and we make a consistency check in a semi-quantitative way.

This paper is organized as follows. In Sec. 2 we will briefly review the field theoretical treatment of rotation and the energy dispersion relation gapped by the causality bound. In Sec. 3 we will set forth our strategy to describe deconfinement within the HRG model based on the Hagedorn picture. In Sec. 4 we will give an explicit expression for the pressure in the rotating frame and spell out calculational procedures. The pressure has explicit dependence on the radial distance from the rotation axis and we closely discuss the physical interpretation in Sec. 5. Section 6 constitutes our central results in this paper and we will show a 3D phase boundary surface as a function of the baryon chemical potential  $\mu$  and the angular velocity  $\omega$ . In Sec. 7 we will revisit the  $r$  dependence to make a consistency check between the physical interpretation and the numerical results. Section 8 is devoted to the summary and outlooks.

## 2. Causality bound in the rotating frame

The most straightforward approach to treat rotating systems is to describe physics in a rotating frame by transforming non-rotating coordinates,  $\bar{x}^\mu$ , into  $x^\mu$  rotating with the angular velocity  $\omega$ . We take the rotation axis along the  $z$  direction, so that local quantities in the rotating frame are given as functions of

$$x = \bar{x} \cos \omega t + \bar{y} \sin \omega t, \quad y = -\bar{x} \sin \omega t + \bar{y} \cos \omega t. \quad (1)$$

We can read the metric as

$$g_{\mu\nu} = \eta_{ab} \frac{\partial \bar{x}^a}{\partial x^\mu} \frac{\partial \bar{x}^b}{\partial x^\nu} = \begin{pmatrix} 1 - (x^2 + y^2)\omega^2 & y\omega & -x\omega & 0 \\ y\omega & -1 & 0 & 0 \\ -x\omega & 0 & -1 & 0 \\ 0 & 0 & 0 & -1 \end{pmatrix}. \quad (2)$$

Here,  $\eta_{ab}$  represents the Minkowskian metric:

$\eta = \text{diag}(1, -1, -1, -1)$ . For the fermionic particles the equations of motion involve the first order derivatives, so we need further to introduce the vierbein,  $\eta_{ab} = e^\mu_a e^\nu_b g_{\mu\nu}$ , where

$$e^t_0 = e^x_1 = e^y_2 = e^z_3 = 1 \quad e^x_0 = y\omega, \quad e^y_0 = -x\omega, \quad (3)$$

and the other components are zero. The explicit calculations<sup>1</sup> using the metric and the vierbein lead to a shift in the Hamiltonian as

$$\hat{H} \rightarrow \hat{H} - \mathbf{J} \cdot \boldsymbol{\omega} \quad (4)$$

in the rotating frame, where  $\mathbf{J}$  is the total angular momentum; namely,  $\mathbf{J} = \mathbf{L} + \mathbf{S}$ , with the orbital part  $\mathbf{L}$  and the spin part  $\mathbf{S}$ . Accordingly the energy dispersion relation for spin- $S$  particles should be shifted as

$$\varepsilon \rightarrow \varepsilon - (\ell + s)\omega. \quad (5)$$

Here,  $s = -S, -S + 1, \dots, S - 1, S$  and  $\ell$  denotes the quantum number corresponding to the  $z$  component of the orbital angular momentum, i.e.,  $L_z$ .

The energy shift above is analogous to the chemical potential for finite density systems:  $(\ell + s)\omega$  can be regarded as an effective chemical potential. Then, one might think that, for  $(\ell + s)\omega > \varepsilon$ , a Bose-Einstein condensate should form for bosons, or, a Fermi surface should appear for fermions. This is, however, unphysical because Eq. (1) is merely a coordinate transformation and the vacuum physics must not change, while the rotation together with external effects such as the temperature, the electromagnetic fields, etc could make physical differences.

In fact,  $(\ell + s)\omega > \varepsilon$  is prohibited by the causality condition. In the cylindrical coordinates  $(r, \varphi, z)$ , we can perform the Bessel-Fourier expansion to define the modes with corresponding momenta,  $(k_r, \ell, k_z)$ , where  $\ell$  is nothing but the orbital angular momentum. We can then impose a boundary condition at  $r = R$ , such that the wavefunctions are normalized within  $r \leq R$ . The causality requires,

$$R\omega \leq 1. \quad (6)$$

We note that the right hand side in the above condition is the speed of light,  $c = 1$ , in the natural unit. The boundary condition at  $r = R$  makes the momenta discretized

<sup>1</sup>We can find explicit calculations for  $S = 0$  and  $S = 1/2$  in the literature: see Ref. [12, 16–18, 33] for several examples, and in the present work we assume that the energy shift by  $-\mathbf{J} \cdot \boldsymbol{\omega}$  generally holds for  $S = 1, 3/2$  and 2 as well.

as  $k_r = \xi_{\ell,n}/R$  with  $\xi_{\ell,n}$  being the  $n$ th zero of the Bessel function:  $J_\ell(\xi_{\ell,n}) = 0$  [12, 18, 34]. It is important to note that  $J_{\ell \geq 1}(\xi)$  has a zero at  $\xi = 0$  but such a zero mode is identically vanishing due to the boundary condition at  $r = R$ , and there is no zero mode contribution to physical quantities. Strictly speaking, thus,  $\xi_{\ell,n}$  indicates the  $n$ th zero excluding a trivial zero at  $\xi = 0$ . In this way we can conclude that the energy is always gapped at least by  $\xi_{\ell,1}/R$  for any particles. We combine this gap and the condition (6) to confirm,

$$\varepsilon \geq \frac{\xi_{\ell,1}}{R} \geq \xi_{\ell,1} \omega. \quad (7)$$

It is known that  $\xi_{\ell,n}$ 's satisfy the following inequality:  $\xi_{\ell,1} > \ell + 1.855757\ell^{1/3} + 0.5\ell^{-1/3}$  for  $\ell \geq 1$  and  $\xi_{0,1} = 2.40483$ . These relations guarantee  $\varepsilon > (\ell + s)\omega$  for sufficiently large  $\ell$  even when  $s$  is large. Our present calculations, as we explain in details later, contain hadrons up to  $S = 2$  and  $\varepsilon > (\ell + s)\omega$  holds for  $|s| \leq S$  and all  $\ell$ .

### 3. Deconfinement transition in the Hagedorn picture

The HRG model analysis is thoroughly hadronic, but we can still discuss the deconfinement transition as follows. Historically speaking, the Hagedorn limiting temperature was first recognized within the framework of hadronic bootstrap model [30]. Later, then, Cabibbo and Parisi realized that the limiting temperature should be given a correct physical interpretation as the transition temperature to more fundamental degrees of freedom than hadrons [31].

Let us suppose that the hadron mass spectrum rises exponentially, i.e.,

$$\rho(m) = e^{m/T_H}, \quad (8)$$

where  $T_H$  is not a physical temperature but just a slope parameter to characterize the mass spectrum. Then, the integration weighted with the Boltzmann factor,  $e^{-m/T}$ , gives us the partition function as

$$Z = \int dm \rho(m) e^{-m/T}. \quad (9)$$

For simplicity we omit the phase space volume (that would give a polynomial factor) and focus on the exponential behavior only. In other words the integration measure of  $dm$  is implicitly defined in a consistent way. Now, it is obvious that the integration diverges for  $T > T_H$ , and Hagedorn considered that  $T_H$  should be the limiting temperature: any physical systems of hadrons cannot be heated above  $T_H$ . This conjecture should be revised once internal structures of hadrons are taken into account. The existence of  $T_H$  should be correctly interpreted as a breakdown point of such a simple hadronic description and the physical systems should be better characterized by quarks and gluons at  $T > T_H$ .

In the HRG model, the hadron mass spectrum is taken from the experimental data, and interestingly,  $\rho(m)$  shows exponential growth up to  $m \sim 3$  GeV. Therefore, the above picture of deconfinement makes approximate sense, and we can see blowup behavior of thermodynamic quantities such as the pressure, the internal energy, the entropy density, and so on at a certain temperature ( $T \sim T_H$ ), though they do not diverge strictly. Therefore, we can physically identify the deconfinement crossover point from the blowup behavior of thermodynamic quantities in the HRG model. It is straightforward to extend the above mentioned picture to a finite density case by replacing the Boltzmann factor with  $e^{-(m-\mu)/T}$  for baryons that also exhibit exponential spectra  $\sim e^{m/T_B}$  (see Ref. [32]). We will explain our working criterion for deconfinement in later discussions.

### 4. Rotating hadron resonance gas model

The HRG model has been well established and for our purpose to investigate rotating systems we need to rewrite the formulas in terms of the cylindrical coordinates,  $(k_r, \ell, k_z)$ . The pressure in the HRG model has contributions from both mesons ( $m$ ) and baryons ( $b$ ) up to an ultraviolet mass scale,  $\Lambda$ :

$$p(T, \mu, \omega; \Lambda) = \sum_{m; M_i \leq \Lambda} p_m + \sum_{b; M_i \leq \Lambda} p_b, \quad (10)$$

The mesonic and the baryonic pressures are given by

$$p_m = p_{i=m}^-, \quad p_b = p_{i=b}^+, \quad (11)$$

where the generalized pressure functions are

$$p_i^\pm = \pm \frac{T}{8\pi^2} \sum_{\ell=-\infty}^{\infty} \int dk_r^2 \int dk_z \sum_{\nu=\ell}^{\ell+2S_i} J_\nu^2(k_r r) \times \log \{1 \pm \exp[-(\varepsilon_{\ell,i} - \mu_i)/T]\}. \quad (12)$$

The energy spectrum is  $\varepsilon_{\ell,i} = \sqrt{k_r^2 + k_z^2 + m_i^2} - (\ell + S_i)\omega$  with  $S_i$  and  $m_i$  being the spin and the mass of the particle  $i$ . We note that the radial integration is with respect to  $k_r^2$  in the above form; that is,  $dk_r^2 = 2k_r dk_r$ . The above expression needs some more explanations. The rotation effect shifts the energy dispersion relation by the cranking term, i.e.,  $-\mathbf{J} \cdot \boldsymbol{\omega}$ , which varies as  $(\ell + s_i)\omega$  from  $s_i = -S_i$  to  $s_i = +S_i$ . We reorganize the sum over  $s_i$  and  $\ell$  so that the energy shift can be the same,  $-(\ell + S_i)\omega$ , to simplify the expression. Then, the spin sum is translated to the sum with respect to  $\nu$  with the square of the Bessel function  $J_\nu^2(k_r r)$  as in Eq. (12). The Bessel function arises from the weight in the Bessel-Fourier expansion. The simplest nontrivial example is the spin-1/2 calculation (see Ref. [18, 35] for more details). After the appropriate redefinition of  $\ell$  in such a way that the total angular momentum is

$j = \ell + 1/2$ , one particle solutions of the Dirac equation read:

$$u_+ = \frac{e^{-i\epsilon t + ik_z z}}{\sqrt{\epsilon + m}} \begin{pmatrix} (\epsilon + m)J_\ell(k_r r)e^{i\ell\varphi} \\ 0 \\ k_z J_\ell(k_r r)e^{i\ell\varphi} \\ ik_r J_{\ell+1}(k_r r)e^{i(\ell+1)\varphi} \end{pmatrix}. \quad (13)$$

The other solution,  $u_-$ , can be expressed similarly (the explicit expression is found in Ref. [18]). From these solutions the fermionic propagator can be constructed and its trace involves  $J_\ell^2(k_r r) + J_{\ell+1}^2(k_r r)$ , that is nothing but the sum we see in Eq. (12) for  $S_i = 1/2$ .

It is important to note that the integrations and the sum in Eq. (12) are convergent. We can understand that from the  $\omega \rightarrow 0$  limit to recover the standard expression in the HRG model:

$$p_i^\pm \rightarrow \pm \frac{g_i T}{2\pi^2} \int_0^\infty k^2 dk \log \left\{ 1 \pm \exp \left[ -\frac{\sqrt{k^2 + m_i^2} - \mu_i}{T} \right] \right\}, \quad (14)$$

where  $g_i = 2S_i + 1$  is the spin degeneracy factor and this expression is certainly convergent. The dispersion relation involves an exponentially growing factor,  $e^{\ell\omega/T}$ , but  $J_{\nu>\ell}^2(k_r r)$  has stronger exponential suppression and Eq. (12) is finite.

There is, however, one subtlety in Eq. (12). As discussed in Sec. 2, we can avoid unphysical condensates from the causality bound, but it is time consuming to take the discrete sum of  $k_r$ . Here, instead, we shall employ an approximate and minimal prescription to evade unphysical condensates. As long as  $\omega$  is not significantly larger than  $\Lambda_{\text{QCD}}$ , the discretization in high momentum regions is expected to be a minor effect, and the leading discretization effect in the low momentum regions is the mass gap. We can thus introduce an infrared cutoff for the  $k_r$  integration,  $\Lambda_\ell^{\text{IR}}$ , defined by

$$\Lambda_\ell^{\text{IR}} = \xi_{\ell,1}\omega, \quad (15)$$

where, as we already noted, an obvious zero at  $\xi = 0$  is excluded. The  $k_r$  integration in Eq. (12) is then replaced as

$$\int dk_r^2 \rightarrow \int_{(\Lambda_\ell^{\text{IR}})^2} dk_r^2. \quad (16)$$

We will elucidate technical procedures in more details in Sec. 6.

## 5. Radial dependence

We note that our main formula (12) depends on the radial coordinate  $r$  through  $J_\nu^2(k_r r)$ . There are twofold intuitive origins for this  $r$  dependence. One is possible  $r$  dependence from the boundary effect at  $R \sim 1/\omega$ . The boundary effect exists even for non-rotating matter. We are interested in not surface singularities (as discussed in Ref. [35] for example) but bulk properties, and so we can take as small  $r$  as possible for numerical implementation.

Another origin is that the centrifugal force should be supported by the  $r$  dependent part of the pressure.

Let us consider the  $r$  dependence from the latter origin. From the analogy to the relation between the baryon number density and the pressure:  $n = \partial p / \partial \mu$ , we can express the angular momentum density as

$$\langle j \rangle(r) = \frac{\partial p(r)}{\partial \omega}. \quad (17)$$

When  $\omega$  is small in the linear regime, the angular momentum is related to the moment of inertia in the infinitesimal volume  $dV$  as

$$\langle j \rangle(r) dV \simeq dI(r)\omega. \quad (18)$$

For homogeneous matter with mass density  $\rho$ , we can easily find the moment of inertia as  $dI(r) = \rho r^2 dV$ . If the baryon chemical potential is vanishing,  $\rho$  should be characterized by the temperature  $T$ , i.e.,  $\rho = \sigma T^4$ . We can roughly approximate  $\sigma$  from the enthalpy density; namely,  $\sigma = 2\nu\pi^2/45$  with the thermal degrees of freedom  $\nu$ . Then, we can approximate:

$$p(r) = p(0) + \Delta p(r), \quad \Delta p(r) \simeq \frac{\sigma}{2} T^4 r^2 \omega^2. \quad (19)$$

Because  $\sigma$  may differ for confined hadronic matter and deconfined matter of quarks and gluons, the deconfinement point could be in principle dependent on  $r$ . Indeed in the cylinder with a boundary, the possibility of spatially separated regions of confinement and deconfinement was pointed out [25].

In the present work, to avoid ambiguous interpretation, we shall take  $r\omega \ll 1$  so that we can safely neglect the  $r$  dependence: we fix  $r = 0.01 \text{ GeV}^{-1}$  throughout this work. If we take the strict limit of  $r \rightarrow 0$  in the integrand in Eq. (12) (assuming that the infinite sum over  $\ell$  and the integration with respect to  $k_r$  are harmless), all the terms involving  $J_{\nu \neq 0}^2(0) = 0$  should vanish. Then, only terms with  $\nu = 0$  survive, which are allowed for  $\ell = -2S_i$  to  $\ell = 0$ , corresponding to the energy shifts from  $-S_i\omega$  to  $+S_i\omega$ . Since we redefined  $\ell$  to simplify Eq. (12), it is a bit nontrivial to see, but the surviving terms are different spin states with zero orbital angular momentum. This is very natural: at  $r = 0$  the orbital angular momentum is identically zero and the rotation couples to the spin only.

## 6. Numerical results

In our HRG model treatment we have adopted the particle data group list of particles contained in the package of THERMUS-V3.0 [36] and incorporated the data into our own numerical codes. To reduce the numerical cost, we impose an ultraviolet mass cutoff as  $\Lambda = 1.5 \text{ GeV}$  in Eq. (12). This also limits the high spin states. With our choice of  $\Lambda = 1.5 \text{ GeV}$  the largest spin states contributing to the pressure are  $f_2(1270)$ ,  $a_2(1320)$ ,  $K_2^*(1430)$ , and  $f_2(1430)$  with  $S = 2$ . The effect of  $\Lambda$  on the chemical freezeout curve has been examined in Ref. [37], and they have found

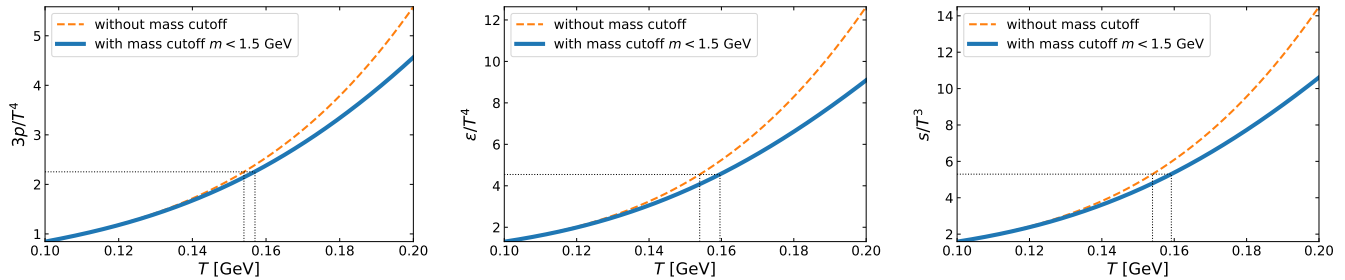


Figure 1: Thermodynamic quantities, the pressure (left), the energy density (middle), and the entropy (right), calculated in the HRG model with and without imposing the mass cutoff  $m < \Lambda$  with  $\Lambda = 1.5$  GeV.

that the changes of the chemical freezeout curve are as small as around 10 MeV.

We quantitatively study the effect of  $\Lambda$ . In Fig. 1 we plot the thermodynamic quantities with and without the cutoff from Eq. (14) in the standard non-rotating HRG model. The left panel shows the pressure  $p$ , the middle shows the energy density  $\varepsilon$ , and the right shows the entropy density  $s$  as functions of  $T$ . To check the validity of our simplification with  $\Lambda$ , we shall compare the critical temperature  $T_c$  read out from a thermodynamic criterion.

The critical temperature without  $\Lambda$  is known from the lattice-QCD simulation as  $T_c = 154$  MeV [38]. We can find the corresponding critical  $p/T^4$ ,  $\varepsilon/T^4$ , and  $s/T^3$  at  $T_c$  from the crossing points of the orange dashed curves and the dotted vertical lines. Then, we can estimate the  $\Lambda$  modified  $T_c$  from the crossing points of the blue solid curves and the dotted horizontal lines in Fig. 1. The shifts in  $T_c$  read out from  $p/T^4$ ,  $\varepsilon/T^4$ , and  $s/T^3$  are 3.0 MeV, 5.6 MeV, and 5.2 MeV, respectively. This is the numerical confirmation that the  $\Lambda$  effects on  $T_c$  are less than 10 MeV. In conclusion, our simplification by  $\Lambda = 1.5$  GeV is qualitatively harmless for the study of the phase boundary around  $T_c$  and also at the quantitative level the possible error is  $\sim 5$  MeV. We assume that the  $\Lambda$  effects are negligible for finite  $\omega$  as well.

Now let us discuss the deconfinement phase boundaries at finite  $\mu$  and  $\omega$ . For this purpose we should make the thermodynamic quantities not only with  $T$  (as in Fig. 1) but with some proper combination of  $T$ ,  $\mu$ , and  $\omega$ . We employ the normalization given by the Stefan-Boltzmann limit of a rotating quark-gluon gas:

$$p_{\text{SB}} \equiv (N_c^2 - 1)p_g + N_c N_f (p_q + p_{\bar{q}}), \quad (20)$$

where the number of colors and flavors are  $N_c = 3$ ,  $N_f = 2$ , respectively. The gluon pressure reads:

$$p_g = -\frac{T}{8\pi^2} \sum_{\ell=-\infty}^{\infty} \int_{\Lambda_{\ell}^{\text{IR}}} dk_r^2 \int dk_z [J_{\ell}^2(k_r, r) + J_{\ell+2}^2(k_r, r)] \times \log \left\{ 1 - \exp \left[ -\frac{\sqrt{k_r^2 + k_z^2} - (\ell + 1)\omega}{T} \right] \right\}. \quad (21)$$

Here, we note that the possible angular momenta are only  $j = \ell - 1$  and  $j = \ell + 1$  and there is no contribution from

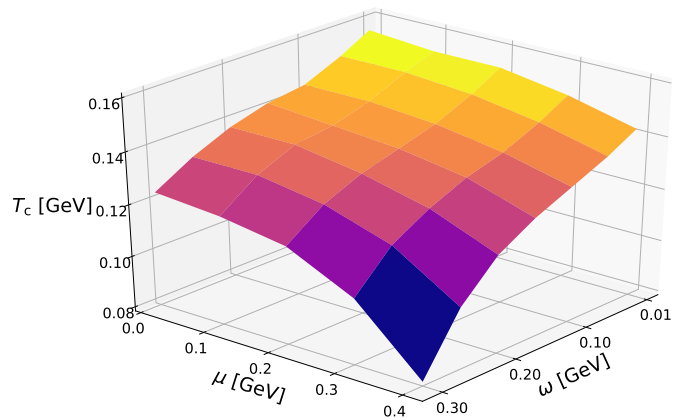


Figure 2: Deconfinement transition surface as a function of the baryon chemical potential  $\mu$  and the angular velocity  $\omega$ .

$s_z = 0$  because gluons are massless gauge bosons. This is why  $J_{\ell}^2(k_r, r) + J_{\ell+2}^2(k_r, r)$  appears above. The quark pressure reads more straightforwardly:

$$p_q = -\frac{T}{8\pi^2} \sum_{\ell=-\infty}^{\infty} \int_{\Lambda_{\ell}^{\text{IR}}} dk_r^2 \int dk_z [J_{\ell}^2(k_r, r) + J_{\ell+1}^2(k_r, r)] \times \log \left\{ 1 + \exp \left[ -\frac{\sqrt{k_r^2 + k_z^2} + (\ell + \frac{1}{2})\omega - \frac{\mu}{N_c}}{T} \right] \right\} \quad (22)$$

and the anti-quark pressure,  $p_{\bar{q}}$ , takes almost the same expression with  $\mu \rightarrow -\mu$ .

Here our criterion for the deconfinement transition is prescribed, in a way similar to Ref. [39], as

$$\frac{p}{p_{\text{SB}}}(T_c, \mu, \omega) = \gamma. \quad (23)$$

Here,  $\gamma$  is a constant, which is chosen to reproduce  $T_c(\mu = \omega = 0) = 154$  MeV in accordance with the lattice-QCD results [38]. This condition fixes  $\gamma = 0.18$  in our calculation. Now we can numerically solve Eq. (23) to identify  $T_c = T_c(\mu, \omega)$  as plotted in Fig. 2.

Now it is evident that  $T_c$  is a decreasing function with increasing  $\omega$  just like the behavior along the  $\mu$  direction. We cannot directly study the chiral properties within the HRG model, but it is conceivable that the deconfinement

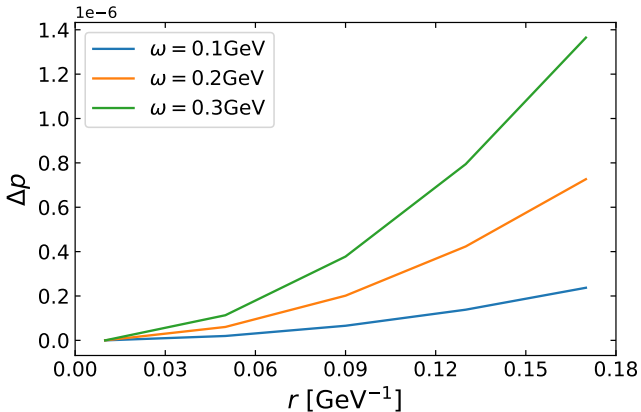


Figure 3:  $\Delta p$  as a function of  $r$  for three different values of  $\omega$ .

$T_c$  and the chiral restoration temperature are linked even at finite  $\omega$ . We can also notice that the effect of  $\omega$  makes  $T_c$  drop faster than that of  $\mu$ . We understand this from the  $\omega$  induced effective chemical potential which is proportional to  $\ell + S_i$ . Because  $\ell$  becomes arbitrarily large, the system can be more sensitive to the effective chemical potential than the baryon chemical potential. From our parameter free analyses we make a conclusion that the deconfining transition temperature is lowered by the rotation effect.

## 7. Revisiting the radial dependence

It would be an interesting problem to make systematic investigations of the  $r$  and  $\omega$  dependence in the pressure. The main focus of the present work is the survey of the phase diagram, so we will not go into systematic discussions here. Still, it would be instructive to verify our physical interpretation of the  $r$  and  $\omega$  dependence in Eq. (19) from the numerical calculation.

We fix the temperature,  $T = 0.15$  GeV, and change  $r$  for three different values of  $\omega = 0.1, 0.2, 0.3$  GeV. The range of  $r$  is  $[0.01, 0.17]$  GeV<sup>-1</sup>. Our numerical calculations lead to the  $r$  dependence as shown in Fig. 3. We have checked that each curve on Fig. 3 is well fitted by a quadratic function  $\propto r^2$  as expected from Eq. (19). From this quadratic  $r$  dependence we can numerically estimate  $\sigma$  defined in Eq. (19). For  $\omega = 0.1$  GeV the numerical coefficient reads:  $\Delta p/r^2 \simeq 8.19141 \times 10^{-6}$  GeV<sup>6</sup>. The corresponding value of  $\sigma$  is  $\sigma \simeq 3.21$ , from which we can infer,

$$\nu(\omega = 0.1 \text{ GeV}) \simeq 7. \quad (24)$$

For different  $\omega$  the results are slightly changed, but of the same order. This value of  $\nu$  is comparable to the thermal degrees of freedom of light mesons, i.e., pions and Kaons. We have a full expression of Eq. (12) and we do not have to rely on an Ansatz like Eq. (19). In this sense the above mentioned estimate of  $\nu$  should be understood as a consistency check. It would be a very intriguing question to see the spatial distribution of the angular momentum density,

$\langle j \rangle(r)$ , as well as the moment of inertia,  $dI(r)$ , directly from Eq. (12). We will report a thorough analysis in a separate publication and stop our discussions at the level of the consistency check in the present paper.

## 8. Summary

We studied the effect of rotation on the deconfinement transition from hadronic to quark matter. We devised the hadron resonance gas (HRG) model in a rotating frame and formulated a practical scheme for the pressure calculation that is dependent on the radial distance  $r$  from the rotation axis. Adopting a working criterion for deconfinement in the view of the Hagedorn picture, we found that increasing the angular velocity  $\omega$  lowers the deconfinement transition temperature, which is similar to the effect of baryon chemical potential. We then drew the 3D phase diagram of rotating hot and dense matter in Fig. 2. Our physics discussions include not only the phase diagram but also the physical interpretation of the spatial dependence of the pressure. The numerical results are consistent with the physical interpretation in terms of the moment of inertia.

There are many interesting directions for future extensions. In the context of the QCD phase diagram research it would provide us with an inspiring insight to study whether the deconfinement and the chiral restoration transitions should be locked or unlocked by rotational effects. Also, a more comprehensive analysis involving the magnetic field on top of rotation would be desirable for phenomenological applications. Since we formulated the pressure as a function of  $r$  and  $\omega$ , it have paved a clear path for the microscopic computation of the angular momentum and the moment of inertia of rotating hot and dense matter. Such quantities should be valuable for phenomenological modeling. We are making progress along these lines using perturbative QCD as well as the HRG model.

## Acknowledgments

This work was supported by Japan Society for the Promotion of Science (JSPS) KAKENHI Grant Nos. 18H01211 (KF,YH), 19K21874 (KF), 17H06462 (YH), and 20J10506 (YF).

## References

- [1] A. Bohr, Rotational motion in nuclei, Rev. Mod. Phys. 48 (1976) 365–374. [doi:10.1103/RevModPhys.48.365](https://doi.org/10.1103/RevModPhys.48.365).
- [2] T. Otsuka, Y. Tsunoda, T. Abe, N. Shimizu, P. Van Duppen, Underlying structure of collective bands and self-organization in quantum systems, Phys. Rev. Lett. 123 (22) (2019) 222502. [arXiv:1907.10759](https://arxiv.org/abs/1907.10759), [doi:10.1103/PhysRevLett.123.222502](https://doi.org/10.1103/PhysRevLett.123.222502).
- [3] K. Fukushima, Extreme matter in electromagnetic fields and rotation, Prog. Part. Nucl. Phys. 107 (2019) 167–199. [arXiv:1812.08886](https://arxiv.org/abs/1812.08886), [doi:10.1016/j.pnpnp.2019.04.001](https://doi.org/10.1016/j.pnpnp.2019.04.001).

- [4] F. Becattini, M. A. Lisa, Polarization and Vorticity in the Quark Gluon Plasma (3 2020). [arXiv:2003.03640](https://arxiv.org/abs/2003.03640), [doi:10.1146/annurev-nucl-021920-095245](https://doi.org/10.1146/annurev-nucl-021920-095245).
- [5] X.-G. Huang, J. Liao, Q. Wang, X.-L. Xia, Vorticity and Spin Polarization in Heavy Ion Collisions: Transport Models (10 2020). [arXiv:2010.08937](https://arxiv.org/abs/2010.08937).
- [6] L. Adamczyk, et al., Global  $\Lambda$  hyperon polarization in nuclear collisions: evidence for the most vortical fluid, *Nature* 548 (2017) 62–65. [arXiv:1701.06657](https://arxiv.org/abs/1701.06657), [doi:10.1038/nature23004](https://doi.org/10.1038/nature23004).
- [7] F. Becattini, G. Inghirami, V. Rolando, A. Beraudo, L. Del Zanna, A. De Pace, M. Nardi, G. Pagliara, V. Chandra, A study of vorticity formation in high energy nuclear collisions, *Eur. Phys. J. C* 75 (9) (2015) 406, [Erratum: *Eur.Phys.J.C* 78, 354 (2018)]. [arXiv:1501.04468](https://arxiv.org/abs/1501.04468), [doi:10.1140/epjc/s10052-015-3624-1](https://doi.org/10.1140/epjc/s10052-015-3624-1).
- [8] Y. Jiang, Z.-W. Lin, J. Liao, Rotating quark-gluon plasma in relativistic heavy ion collisions, *Phys. Rev. C* 94 (4) (2016) 044910, [Erratum: *Phys.Rev.C* 95, 049904 (2017)]. [arXiv:1602.06580](https://arxiv.org/abs/1602.06580), [doi:10.1103/PhysRevC.94.044910](https://doi.org/10.1103/PhysRevC.94.044910).
- [9] W.-T. Deng, X.-G. Huang, Vorticity in Heavy-Ion Collisions, *Phys. Rev. C* 93 (6) (2016) 064907. [arXiv:1603.06117](https://arxiv.org/abs/1603.06117), [doi:10.1103/PhysRevC.93.064907](https://doi.org/10.1103/PhysRevC.93.064907).
- [10] A. Vilenkin, Parity Violating Currents in Thermal Radiation, *Phys. Lett. B* 80 (1978) 150–152. [doi:10.1016/0370-2693\(78\)90330-1](https://doi.org/10.1016/0370-2693(78)90330-1).
- [11] A. Vilenkin, MACROSCOPIC PARITY VIOLATING EFFECTS: NEUTRINO FLUXES FROM ROTATING BLACK HOLES AND IN ROTATING THERMAL RADIATION, *Phys. Rev. D* 20 (1979) 1807–1812. [doi:10.1103/PhysRevD.20.1807](https://doi.org/10.1103/PhysRevD.20.1807).
- [12] A. Vilenkin, QUANTUM FIELD THEORY AT FINITE TEMPERATURE IN A ROTATING SYSTEM, *Phys. Rev. D* 21 (1980) 2260–2269. [doi:10.1103/PhysRevD.21.2260](https://doi.org/10.1103/PhysRevD.21.2260).
- [13] D. T. Son, P. Surowka, Hydrodynamics with Triangle Anomalies, *Phys. Rev. Lett.* 103 (2009) 191601. [arXiv:0906.5044](https://arxiv.org/abs/0906.5044), [doi:10.1103/PhysRevLett.103.191601](https://doi.org/10.1103/PhysRevLett.103.191601).
- [14] Y. Liu, I. Zahed, Pion Condensation by Rotation in a Magnetic field, *Phys. Rev. Lett.* 120 (3) (2018) 032001. [arXiv:1711.08354](https://arxiv.org/abs/1711.08354), [doi:10.1103/PhysRevLett.120.032001](https://doi.org/10.1103/PhysRevLett.120.032001).
- [15] Y. Liu, I. Zahed, Rotating Dirac fermions in a magnetic field in 1+2 and 1+3 dimensions, *Phys. Rev. D* 98 (1) (2018) 014017. [arXiv:1710.02895](https://arxiv.org/abs/1710.02895), [doi:10.1103/PhysRevD.98.014017](https://doi.org/10.1103/PhysRevD.98.014017).
- [16] H.-L. Chen, K. Fukushima, X.-G. Huang, K. Mameda, Analogy between rotation and density for Dirac fermions in a magnetic field, *Phys. Rev. D* 93 (10) (2016) 104052. [arXiv:1512.08974](https://arxiv.org/abs/1512.08974), [doi:10.1103/PhysRevD.93.104052](https://doi.org/10.1103/PhysRevD.93.104052).
- [17] Y. Jiang, J. Liao, Pairing Phase Transitions of Matter under Rotation, *Phys. Rev. Lett.* 117 (19) (2016) 192302. [arXiv:1606.03808](https://arxiv.org/abs/1606.03808), [doi:10.1103/PhysRevLett.117.192302](https://doi.org/10.1103/PhysRevLett.117.192302).
- [18] S. Ebihara, K. Fukushima, K. Mameda, Boundary effects and gapped dispersion in rotating fermionic matter, *Phys. Lett. B* 764 (2017) 94–99. [arXiv:1608.00336](https://arxiv.org/abs/1608.00336), [doi:10.1016/j.physletb.2016.11.010](https://doi.org/10.1016/j.physletb.2016.11.010).
- [19] M. Chernodub, S. Gongyo, Interacting fermions in rotation: chiral symmetry restoration, moment of inertia and thermodynamics, *JHEP* 01 (2017) 136. [arXiv:1611.02598](https://arxiv.org/abs/1611.02598), [doi:10.1007/JHEP01\(2017\)136](https://doi.org/10.1007/JHEP01(2017)136).
- [20] M. Chernodub, S. Gongyo, Effects of rotation and boundaries on chiral symmetry breaking of relativistic fermions, *Phys. Rev. D* 95 (9) (2017) 096006. [arXiv:1702.08266](https://arxiv.org/abs/1702.08266), [doi:10.1103/PhysRevD.95.096006](https://doi.org/10.1103/PhysRevD.95.096006).
- [21] X. Wang, M. Wei, Z. Li, M. Huang, Quark matter under rotation in the NJL model with vector interaction, *Phys. Rev. D* 99 (1) (2019) 016018. [arXiv:1808.01931](https://arxiv.org/abs/1808.01931), [doi:10.1103/PhysRevD.99.016018](https://doi.org/10.1103/PhysRevD.99.016018).
- [22] H. Zhang, D. Hou, J. Liao, Mesonic Condensation in Isospin Matter under Rotation, *Chin. Phys. C* 44 (11) (2020) 111001. [arXiv:1812.11787](https://arxiv.org/abs/1812.11787), [doi:10.1088/1674-1137/abae4d](https://doi.org/10.1088/1674-1137/abae4d).
- [23] V. V. Braguta, A. Y. Kotov, D. D. Kuznedev, A. A. Roenko, Study of the confinement/deconfinement phase transition in rotating lattice  $su(3)$  gluodynamics, *JETP Letters* 112 (1) (2020) 6–12. [doi:10.1134/S0021364020130044](https://doi.org/10.1134/S0021364020130044) URL <https://doi.org/10.1134/S0021364020130044>
- [24] X. Chen, L. Zhang, D. Li, D. Hou, M. Huang, Gluodynamics and deconfinement phase transition under rotation from holography (10 2020). [arXiv:2010.14478](https://arxiv.org/abs/2010.14478).
- [25] M. Chernodub, Inhomogeneous confining-deconfining phases in rotating plasmas (12 2020). [arXiv:2012.04924](https://arxiv.org/abs/2012.04924).
- [26] A. Yamamoto, Y. Hirono, Lattice QCD in rotating frames, *Phys. Rev. Lett.* 111 (2013) 081601. [arXiv:1303.6292](https://arxiv.org/abs/1303.6292), [doi:10.1103/PhysRevLett.111.081601](https://doi.org/10.1103/PhysRevLett.111.081601).
- [27] A. Andronic, P. Braun-Munzinger, K. Redlich, J. Stachel, Decoding the phase structure of QCD via particle production at high energy, *Nature* 561 (7723) (2018) 321–330. [arXiv:1710.09425](https://arxiv.org/abs/1710.09425), [doi:10.1038/s41586-018-0491-6](https://doi.org/10.1038/s41586-018-0491-6).
- [28] A. Andronic, P. Braun-Munzinger, J. Stachel, M. Winn, Interacting hadron resonance gas meets lattice QCD, *Phys. Lett. B* 718 (2012) 80–85. [arXiv:1201.0693](https://arxiv.org/abs/1201.0693), [doi:10.1016/j.physletb.2012.10.001](https://doi.org/10.1016/j.physletb.2012.10.001).
- [29] V. Vovchenko, D. V. Anchishkin, M. I. Gorenstein, Hadron Resonance Gas Equation of State from Lattice QCD, *Phys. Rev. C* 91 (2) (2015) 024905. [arXiv:1412.5478](https://arxiv.org/abs/1412.5478), [doi:10.1103/PhysRevC.91.024905](https://doi.org/10.1103/PhysRevC.91.024905).
- [30] R. Hagedorn, Statistical thermodynamics of strong interactions at high-energies, *Nuovo Cim. Suppl.* 3 (1965) 147–186.
- [31] N. Cabibbo, G. Parisi, Exponential Hadronic Spectrum and Quark Liberation, *Phys. Lett. B* 59 (1975) 67–69. [doi:10.1016/0370-2693\(75\)90158-6](https://doi.org/10.1016/0370-2693(75)90158-6).
- [32] A. Andronic, et al., Hadron Production in Ultra-relativistic Nuclear Collisions: Quarkyonic Matter and a Triple Point in the Phase Diagram of QCD, *Nucl. Phys. A* 837 (2010) 65–86. [arXiv:0911.4806](https://arxiv.org/abs/0911.4806), [doi:10.1016/j.nuclphysa.2010.02.005](https://doi.org/10.1016/j.nuclphysa.2010.02.005).
- [33] V. E. Ambrus, E. Winstanley, Rotating quantum states, *Phys. Lett. B* 734 (2014) 296–301. [arXiv:1401.6388](https://arxiv.org/abs/1401.6388), [doi:10.1016/j.physletb.2014.05.031](https://doi.org/10.1016/j.physletb.2014.05.031).
- [34] V. E. Ambrus, E. Winstanley, Rotating fermions inside a cylindrical boundary, *Phys. Rev. D* 93 (10) (2016) 104014. [arXiv:1512.05239](https://arxiv.org/abs/1512.05239), [doi:10.1103/PhysRevD.93.104014](https://doi.org/10.1103/PhysRevD.93.104014).
- [35] H.-L. Chen, K. Fukushima, X.-G. Huang, K. Mameda, Surface Magnetic Catalysis, *Phys. Rev. D* 96 (5) (2017) 054032. [arXiv:1707.09130](https://arxiv.org/abs/1707.09130), [doi:10.1103/PhysRevD.96.054032](https://doi.org/10.1103/PhysRevD.96.054032).
- [36] S. Wheaton, J. Cleymans, THERMUS: A Thermal model package for ROOT, *Comput. Phys. Commun.* 180 (2009) 84–106. [arXiv:hep-ph/0407174](https://arxiv.org/abs/hep-ph/0407174), [doi:10.1016/j.cpc.2008.08.001](https://doi.org/10.1016/j.cpc.2008.08.001).
- [37] J. Cleymans, H. Oeschler, K. Redlich, S. Wheaton, Comparison of chemical freeze-out criteria in heavy-ion collisions, *Phys. Rev. C* 73 (2006) 034905. [arXiv:hep-ph/0511094](https://arxiv.org/abs/hep-ph/0511094), [doi:10.1103/PhysRevC.73.034905](https://doi.org/10.1103/PhysRevC.73.034905).
- [38] A. Bazavov, et al., Equation of state in (2+1)-flavor QCD, *Phys. Rev. D* 90 (2014) 094503. [arXiv:1407.6387](https://arxiv.org/abs/1407.6387), [doi:10.1103/PhysRevD.90.094503](https://doi.org/10.1103/PhysRevD.90.094503).
- [39] K. Fukushima, Phase diagram of hot and dense QCD constrained by the Statistical Model, *Phys. Lett. B* 695 (2011) 387–391. [arXiv:1006.2596](https://arxiv.org/abs/1006.2596), [doi:10.1016/j.physletb.2010.11.040](https://doi.org/10.1016/j.physletb.2010.11.040).